

# Magnetohydrodynamic Effects in Propagating Relativistic Ejecta: Reverse Shock and Magnetic Acceleration

Y. Mizuno\*, B. Zhang†, B. Giacomazzo\*\*, K.-I. Nishikawa\*, P. E. Hardee‡, S. Nagataki§ and D. H. Hartmann¶

\*CSPAR, University of Alabama in Huntsville, NSSTC, Huntsville, AL 35805, USA

†Department of Physics and Astronomy, University of Nevada, Las Vegas, NV 89154, USA

\*\*Max-Planck-Institut für Gravitationsphysik, Albert-Einstein-Institut, Potsdam-Golm, Germany

‡Department of Physics and Astronomy, University of Alabama, Tuscaloosa, AL 35487, USA

§Yukawa Institute for Theoretical Physics, Kyoto University, Sakyo, Kyoto, Japan

¶Department of Physics and Astronomy, Clemson University, Clemson, SC 29634, USA

**Abstract.** We solve the Riemann problem for the deceleration of arbitrarily magnetized relativistic ejecta injected into a static unmagnetized medium. We find that for the same initial Lorentz factor, the reverse shock becomes progressively weaker with increasing magnetization  $\sigma$  (the Poynting-to-kinetic energy flux ratio), and the shock becomes a rarefaction wave when  $\sigma$  exceeds a critical value,  $\sigma_c$ , defined by the balance between the magnetic pressure in the ejecta and the thermal pressure in the forward shock. In the rarefaction wave regime, we find that the rarefied region is accelerated to a Lorentz factor that is significantly larger than the initial value. This acceleration mechanism is due to the strong magnetic pressure in the ejecta.

**Keywords:** GRBs, MHD, Riemann Problem, Reverse Shock

## INTRODUCTION

Relativistic jets are believed to exist in active galactic nuclei (AGNs), black hole binaries, and gamma-ray bursts (GRBs), but their composition is still poorly understood. It has been argued that magnetic fields could play an important dynamic role in these jets [1, 2, 3, 4], but the degree of magnetization, quantified by the magnetization parameter  $\sigma$  (the ratio of electromagnetic to kinetic energy flux), is poorly constrained by observations. GRB afterglow modeling indicates that the ejecta are more magnetized than the ambient medium, suggesting a possibly important dynamic role for magnetic fields in GRB jets [5, 6, 7, 8]. A useful diagnostic for the degree of jet-magnetization can be obtained from the interaction between the decelerating jet and the ambient medium. Added magnetic field pressure in the jet alters the condition for formation of a reverse shock (RS) as well as its strength [9]. Analytical studies of the deceleration of a GRB fireball with arbitrary magnetization [10] suggest novel behavior that does not exist in pure hydrodynamic (HD) ( $\sigma = 0$ ) models [11, 12]. However, consensus on the conditions required for the existence of the RS or how Poynting flux is transferred to kinetic flux in the interaction region has not yet been achieved [10, 13, 14]. We present a one-dimensional study of the interaction between a magnetized relativistic flow and a static, unmagnetized external medium. A Riemann problem is solved analytically over a broad range of  $\sigma$ .

## RIEMANN PROBLEM

We consider a Riemann problem consisting of two uniform initial states (left and right) with discontinuous hydrodynamic properties specified by the rest-mass density  $\rho$ , gas pressure  $p$ , specific internal energy  $u$ , specific enthalpy  $h \equiv 1 + u/\rho c^2 + p/\rho c^2$ , and normal velocity  $v^N$ . The right state (the medium external to the ejecta) is assumed to be a cold fluid with constant density, at rest. Specifically, we select the initial conditions:  $\rho_R = 1.0\rho_0$ ,  $p_R = 10^{-2}\rho_0 c^2$ ,  $v_R^N = v_R^x = 0.0$ , where  $\rho_0$  is an arbitrary normalization constant (our simulations are scale-free) and  $c$  is the speed of light. The left state (the propagating relativistic ejecta) is assumed to have a higher density and pressure than the right state, as well as a relativistic velocity. Specifically,  $\rho_L = 10^2\rho_0$ ,  $p_L = 1.0\rho_0 c^2$ , and  $v_L^N = v_L^x = 0.995c$  ( $\gamma_L \simeq 10$ ). The fluid is described by an adiabatic equation of state  $p \propto \rho^\Gamma$  with  $\Gamma = 4/3$ .

To investigate the effects of magnetic fields, we consider a perpendicular field component in the ejecta with  $B^y = 31.623, 100.0, 316.23$ , and  $447.21$  in units of  $(4\pi\rho_0 c^2)^{1/2}$  measured in the laboratory frame, corresponding to  $\sigma \equiv B^2/4\pi\gamma^2 h \rho c^2 \simeq B^2/4\pi\gamma^2 \rho c^2$  being  $0.1, 1.0, 10.0$ , and  $20.0$ , respectively. This field is motivated by the predicted

toroidal field domination at the deceleration radius for GRB outflows [10]. Increasing  $\sigma$  increases the total (kinetic plus magnetic) energy density of the left (ejecta) state.

## RESULTS

We calculate exact solutions of this problem, using the code of Giacomazzo & Rezzolla (2006) [15], in the region  $0.8 \leq x \leq 1.2$  with an initial discontinuity at  $x = 1.0$ , where  $x$  is in arbitrary units [16].

For  $\sigma = 0.1$ , the solution shows a right-moving fast shock (FS: forward shock;  $S_{\rightarrow}$ ), a left-moving fast shock (RS: reverse shock;  $S_{\leftarrow}$ ) relative to the contact discontinuity ( $C$ ). For  $\sigma = 1.0$ , the solution shows similar profiles ( $SCS_{\rightarrow}$ ) as for  $\sigma = 0.1$ . The FS is stronger (due to a higher jump in pressure) and slower (more deceleration relative to the frame of the contact discontinuity), while the RS is weaker but faster. These features are expected from analytical work [10, 14], and agree with 1-D relativistic MHD simulations [17, 18]. When the magnetization of the flow exceeds  $\sigma = 2.7$ , the shock profiles change drastically. For  $\sigma = 10.0$  and  $\sigma = 20.0$ , a prominent left-going rarefaction wave ( $R_{\leftarrow}$ ) is observed, instead of a left-going shock. When the rarefaction wave propagates into the ejecta, density and gas pressure decrease, and the flow velocity increases. The terminal Lorentz factor of the left (ejecta) state and the FS region reaches  $\gamma \sim 14$  for  $\sigma = 10$  and  $\gamma > 16$  for  $\sigma = 20$ . This *magnetic acceleration* mechanism stems from the magnetic pressure in the ejecta<sup>1</sup>.

This magnetic acceleration mechanism is solely an MHD effect and a strong magnetic field is required to generate the rarefaction wave. This is different from the HD/MHD boost mechanism [20, 21].

In the reverse shock cases ( $\sigma = 0.1, 1$ ), the upstream magnetic pressure is lower than the gas pressure in the forward shock, while in the rarefaction wave cases ( $\sigma = 10, 20$ ), the upstream magnetic pressure exceeds the gas pressure in the FS. Thus, the balance between the upstream magnetic pressure in the unshocked ejecta region and the FS gas pressure in the shocked medium [10, 19] provides the condition separating the two regimes. This condition can be derived analytically. For the interaction between relativistic ejecta and an external medium, there exist four physically distinct regions: (1) unshocked medium, (2) shocked medium, (3) shocked ejecta, and (4) unshocked ejecta. A critical  $\sigma_c$  value is given as  $\sigma_c = 2\rho_1(\gamma_4 - 1)(4\gamma_4 + 3)/3\rho_4 \simeq 8\rho_1\gamma_4^2/3\rho_4$ . The condition for the existence of a reverse shock is  $\sigma < \sigma_c$ . The condition for a rarefaction wave and magnetic acceleration is  $\sigma > \sigma_c$ . We adopted  $\rho_1 = \rho_R = 1.0$ ,  $\rho_4 = \rho_L = 10^2$ , and  $\gamma_4 = \gamma_L = 10.0$ , so that the critical value is  $\sigma_c \simeq 2.7$ . Our calculations indicate that  $\sigma_c$  marks the transition point where neither a reverse shock nor a rarefaction wave is established.

To better understand the magnetic acceleration mechanism, we plot the Lorentz factor as a function of  $\sigma$  in Fig.1(a). For the magnetic acceleration case, this is the terminal Lorentz factor after acceleration. Because of the dependence of  $\sigma_c$  on  $\gamma_L$ , a higher  $\sigma$  is needed to achieve acceleration for a higher  $\gamma_L$ . The terminal Lorentz factor can be estimated analytically by requiring that the thermal pressure in the FS region balance the magnetic pressure in the region through which the rarefaction wave has propagated. For the terminal Lorentz factor  $\gamma_t$ , this condition can be expressed roughly as  $\gamma_t \simeq (3\gamma_4^2\sigma\rho_4/8\rho_1)^{1/4}$ . Crosses in Fig.1(a) denote values of estimated terminal Lorentz factors for model parameters,  $\gamma_4 = \gamma_L = 20$ ,  $\rho_1 = \rho_R = 1.0$ , and  $\rho_4 = \rho_L = 10^2$ , in good agreement with the exact solution of the Riemann problem in the reverse rarefaction wave regime.

To investigate the acceleration efficiency, we present in Fig. 1(b) the terminal Lorentz factor  $\gamma_t$ , and its ratio to the initial Lorentz factor ( $\gamma_t/\gamma_L$ ) as a function of the initial ejecta Lorentz factor  $\gamma_L$ . While a ejecta with a higher initial Lorentz factor reaches a higher terminal Lorentz factor, a lower initial Lorentz factor implies a higher acceleration efficiency. From the equation for the terminal Lorentz factor, it follows that  $\gamma_t/\gamma_4 \simeq (3\sigma\rho_4/8\rho_1)^{1/4}\gamma_4^{-1/2}$ , in good agreement with the exact solution of the Riemann problem in relativistic regime.

## DISCUSSION

Our results have implications for understanding deceleration of strongly magnetized outflows, possibly present in GRBs and AGNs. Exact solutions indicate that the condition for the existence of a reverse shock is  $\sigma < \sigma_c$  [10, 14]. The paucity of bright optical flashes in GRBs [22] may, among other interpretations, be attributed to highly magnetized flows. Furthermore, the magnetic acceleration mechanism discussed here suggests that  $\sigma$  and  $\gamma$  are not independent parameters at the deceleration radius. For high- $\sigma$  flows, the ejecta would experience magnetic acceleration at small

---

<sup>1</sup> We note that Romero et al. (2005) [19] also discovered the rarefaction wave regime discussed in this paper, but did not investigate the magnetic acceleration mechanism and its astrophysical implications in detail.

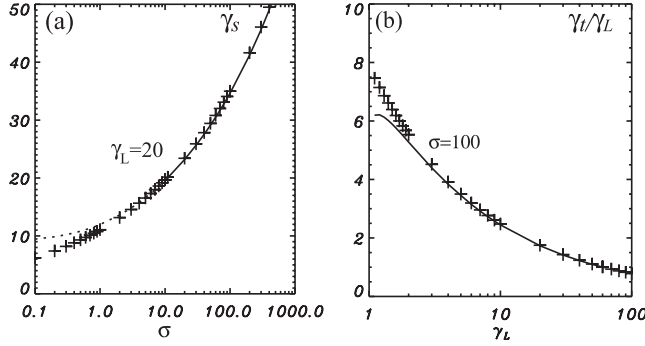


**FIGURE 1.** (a) The  $\sigma$ -dependence of the maximum Lorentz factor in the shocked region in the case with initial Lorentz factor  $\gamma_L = 20$ . (b) The dependence of the acceleration efficiency  $\gamma_t/\gamma_L$  on the initial Lorentz factor  $\gamma_L$  with initial magnetization  $\sigma = 100$ . Solid lines refer to the RR regime and dotted lines to the RS regime obtained with the exact solution. Crosses are the values of the estimated terminal Lorentz factor (left panel) and acceleration efficiency (right panel).

radii, before reaching the coasting regime, so that the coasting Lorentz factor (i.e., the “initial” Lorentz factor for the afterglow) is at least the “terminal” Lorentz factor. Here we only focus on 1-D models with Cartesian geometry. Implications for GRB models will be discussed in more detail when this Riemann problem is solved in conical jet geometry.

## ACKNOWLEDGMENTS

Y.M. acknowledge NASA NNG05GB67G, NNG05GB68G, and NNX08AE57A for partial support during stay at UNLV and partial support by NSF AST-0506719, AST-0506666, NASA NNG05GK73G, NNX07AJ88G, and NNX08AG83G.

## REFERENCES

1. R.D. Blandford, & R.L. Znajek, *MNRAS* **179**, 433 (1977).
2. R.D. Blandford, & D.G. Payne, *MNRAS* **199**, 883 (1982).
3. V.V. Usov, *Nature* **357**, 472 (1992).
4. P. Mészáros, & M.J. Rees, *ApJ* **482**, L29 (1997).
5. Y.-Z. Fan, Z.-G. Dai, Y.-F. Huang, & T. Lu, *CJAA* **2**, 449 (2002).
6. B. Zhang, S. Kobayashi, & P. Mészáros, *ApJ* **595**, 950 (2003).
7. P. Kumar, & A. Panaiteescu, *MNRAS* **346**, 905 (2003).
8. A. Gomboc, et al. *ApJ* **687**, 443 (2008).
9. C.F. Kennel, & F.V. Coroniti, *ApJ* **283**, 694 (1984).
10. B. Zhang, & S. Kobayashi, *ApJ* **628**, 315 (2005).
11. R. Sari, & T. Piran, *ApJ* **455**, L143 (1995).
12. S. Kobayashi, T. Piran, & R. Sari, *ApJ* **513**, 669 (1999).
13. M. Lyutikov, *New J. Phys.* **8**, 119 (2006).
14. D. Giannios, P. Mimica, & M.A. Aloy, *A&A* **478**, 747 (2008).
15. B. Giacomazzo, & L. Rezzolla, *J. Fluid Mech.* **562**, 223 (2006).
16. Y. Mizuno, B. Zhang, B. Giacomazzo, K.-I. Nishikawa, P.E. Hardee, S. Nagataki, & D.H. Hartmann, *ApJ* **690**, L47 (2009).
17. P. Mimica, M.A. Aloy, & E. Müller, *A&A* **466**, 93 (2007).
18. P. Mimica, D. Giannios, & M.A. Aloy, *A&A* in press (2009).
19. R. Romero, J.M. Martí, J.A. Pons, J.M. Ibáñez, & J.A. Miralles, *J. Fluid Mech.* **544**, 323 (2005).
20. M.A. Aloy, & L. Rezzolla, *ApJ* **640**, L115 (2006).
21. Y. Mizuno, P. Hardee, D.H. Hartmann, K.-I. Nishikawa, & B. Zhang, *ApJ* **672**, 72 (2008).
22. P.W.A. Roming, et al., *ApJ* **652**, 1416 (2006).